

CROSS-AXIS SENSITIVITY OF ACCELEROGRAPHS WITH PENDULUM LIKE TRANSDUCERS—MATHEMATICAL MODEL AND THE INVERSE PROBLEM

MARIA I. TODOROVSKA *

Civil and Environmental Engineering Department, University of Southern California, Los Angeles, CA 90089-2531, U.S.A.

SUMMARY

A mathematical model for a three-component accelerograph is presented that accounts for the effects of transducer misalignment and cross-axis sensitivity. The former refers to departures in the alignment of the transducer penduli (typically of the order of few degrees) from an ideal orthogonal system, and the latter to a transducer recording components of motion in directions other than its principal sensitivity axis. Transducer misalignment magnifies the effects of cross-axis sensitivity. These effects are significant only for large amplitude recordings (peak acceleration close to $1g$), for example in the near-field of the 1994 Northridge, California, earthquake. The misalignment angles and the angular amplification constant can be determined by a static tilt test, performed in the field, and solving a generalized inverse problem. This paper presents an algorithm for solution of this inverse problem on a routine basis. Practical implementation of the algorithm and results for 76 instruments of the Los Angeles Strong Motion Array are presented in a separate paper. © 1998 John Wiley & Sons, Ltd.

KEY WORDS: instrumentation; accelerographs; strong earthquake motion recording; data processing; instrument correction; cross-axis sensitivity; misalignment

INTRODUCTION

Accurate recording and processing^{1,2} of strong earthquake motion in the free-field and in structures is important for a variety of studies in earthquake engineering and engineering seismology (e.g., earthquake source mechanism studies, development of scaling models for prediction of various characteristics of strong ground motion, analyses of response of engineered structures and in system identification). It is intrinsic to every physical measurement that it is affected, to some degree, by the characteristics of the measuring device (sensors and recording system), and also by the data-processing techniques. Reconstruction of the measured quantity from the recorded data requires postulating a realistic mathematical model of the measuring device, detailed calibration, and analysis of noise.^{3–15} In the case of strong earthquake motion, the final result is acceleration time history, with large signal-to-noise ratio in a specified frequency interval, then used to calculate velocity and displacement, and Fourier and response spectra, all distributed in digital form.^{16,17}

One ‘imperfection’ of accelerographs with pendulum like transducers is cross-axis sensitivity, which is amplified by transducer misalignment (the principal sensitivity axes of the transducers are not parallel to their nominal directions). This paper presents a mathematical model for one such accelerograph and an algorithm for measuring the misalignment angles. Errors in strong motion data caused by the associated effects were previously addressed by Skinner and Stephenson,¹⁸ and by Wong and Trifunac.¹⁹ The latter derived the equations of motion for the transducer, and illustrated the effects of cross-axis sensitivity and misalignment

* Correspondence to: Maria I. Todorovska, Civil and Environmental Engineering Department, University of Southern California, Los Angeles, CA 90089-2531, U.S.A.

for two example accelerograms. They concluded that, for accelerations ranging from about $0.05g$ to about $1g$ (g is the acceleration due to gravity) the change of amplitude of acceleration due to cross-axis sensitivity for perfectly aligned transducers is of the order of 0.1 per cent to about 3 per cent, and for nonaligned transducers and for typical misalignment angles, of the order of 0.5 per cent to about 5 per cent. Since their work, this problem has received little attention, because not many large accelerations were recorded, until recently. During the Northridge, California, earthquake of 17 January 1994 ($M_L = 6.7$), accelerations close to and exceeding $1g$ were recorded,²⁰ mostly by analogue accelerographs, thus requiring correction for transducer misalignment and cross-axis sensitivity.

The mathematical model in this paper follows the work of Wong and Trifunac,¹⁹ but is presented for different orientation of the co-ordinate axes, to be consistent with strong motion accelerographs of Los Angeles Array.²¹ The proposed algorithm for measuring the transducer misalignment angles and sensitivity is new. It exploits the redundancy of the test measurements and has been developed for routine analysis of test results. Also, it does not require that the tilt table, used to test the instrument, be perfectly horizontal, a requirement which is time consuming to implement in field conditions. Based on the new algorithm, an interactive computer program (TILT) was written for routine processing of test results.²¹ This program also corrects for inclined incidence of light beam onto the film, which is important for accurate estimates of the transducer sensitivity. Using this program, the misalignment angles and sensitivity constants were measured for the Los Angeles Strong Motion Network.^{21,22} The results of this experiment show the range of values for the misalignment angles for a typical strong motion array.

Based on the mathematical model presented in this paper an algorithm for correction of accelerograms for the effects of misalignment and cross-axis sensitivity was developed²¹ and incorporated in the standard data processing programs of Lee and Trifunac.² An analysis of the significance of these corrections²¹ shows that these effects distort the recorded acceleration time series, and cause long period errors in the calculated velocities and displacements. While the change in peak values is, in general, not large, the long period errors in displacement may be important in applications such as system identification and analysis of differential motions, for example. Correcting the errors caused by misalignment and cross-axis sensitivity is also important in applications that require combination of the recorded components of motion, such as computation of rotational components of motion, or of motions in some general direction.

MATHEMATICAL MODEL

Design outline of an accelerograph

Mutatis mutandis, the following will apply to any accelerograph with pendulum-like transducers. To be specific, an SMA-1 accelerograph³ was chosen, which makes the derived equations directly applicable to the Los Angeles Strong Motion Array.^{21,22} An SMA-1 accelerograph has three transducers, measuring motion in three perpendicular directions (L , T and V), which are approximately parallel to the edges of the instrument box ($8 \times 8 \times 14$ in). Ground acceleration in positive L , T and V directions results in upward (positive) trace deflection on the film. Figure 1 shows a view from above of the box with the cover removed, and Figure 2 a transducer removed from the box.

The transducer consists of a plastic plate cantilevered by two leaf springs. Damping, proportional to velocity, is provided by a coil attached to the plate and placed inside a permanent magnetic field. The transducer can be modelled as a single-degree-of-freedom oscillator, i.e. a physical pendulum with mass m , arm r , spiral stiffness K and spiral damping C . Nominal values for the natural frequency $\omega_N = K/(mr^2)$ and the damping ratio ζ ($2\omega_N\zeta = C/(mr^2)$) are $25 \text{ Hz} \times 2\pi \text{ rad} = 50\pi \text{ rad/s}$ and 0.6 (± 0.05) of critical. Light is provided by a bulb attached to the instrument box. For each transducer, by a system of fixed mirrors, a light beam is directed toward a small mirror, attached to and moving with the transducer pendulum (Figures 2 and 3). If the pendulum rotates by an angle α , after reflection from this mirror, the light beam is rotated by 2α . By a fixed mirror, the light beam is reflected back to the moving mirror. After the second reflection, the light beam is again rotated by angle 2α ; the total rotation relative to the incident ray is 4α . By a cylindrical lens, the light

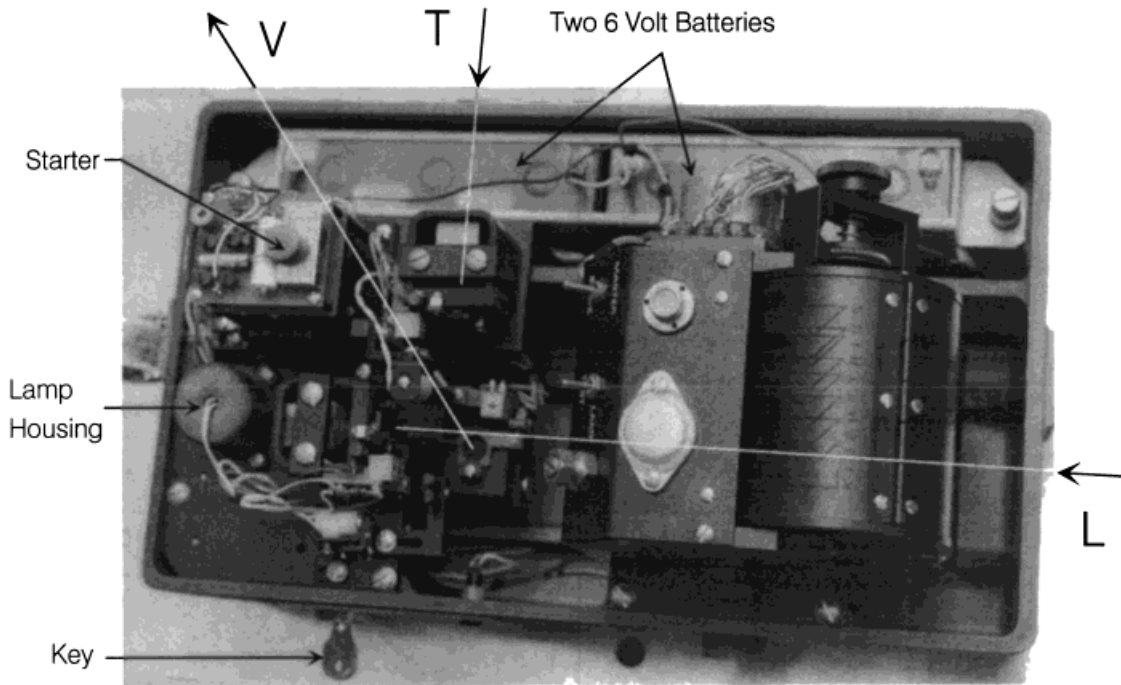


Figure 1. An SMA-1 strong motion accelerograph (a view from above, with the top cover removed)

beam is focused onto the film (70 mm wide) through a thin slit. The total path of the light beam between the mirror attached to the transducer and just before reaching the film (the optical path) is $d = 12.5$ cm (nominal value). If in no load condition, the light beam is perpendicular to the film and

$$\tan 4\alpha = \frac{y}{d}. \tag{1}$$

The transducer response is proportional to the ground acceleration in the frequency range from 0 to about 25 Hz. The overall sensitivity is about 1.7 cm/g (1g acceleration in the direction of the sensitivity axis results in $y = 1.7$ cm trace deflection on the film). The angle α is small, of the order of few degrees (1g acceleration along the sensitivity axis results in $\tan 4\alpha = 1.7/12.5 = 0.136$ or $\alpha = 1.9^\circ$).

Equations of motion for small deflections and perfectly aligned transducers

Figure 4 shows a schematic representation of the transducers inside the box. The penduli are represented by rectangular plates, and the pivot axes by short line segments with circles at the ends. This representation is convenient to verify the directions and signs in the mathematical model with respect to the actual configuration. Ideally, the sensitivity axes should be parallel to the edges of the box.

Indices $i = 1, 2$ and 3 are assigned to the L , T and V transducers, respectively. Further, axes X_1 , X_2 and X_3 are introduced, parallel to the L , T and V axes, but pointing in the opposite direction (Figure 4). The angles of deflection α_i , $i = 1, 2$ and 3 , are shown in Figure 4 by vectors with double arrows. Positive α_i results in upward trace deflection on the film (positive y_i). Axes X_1 , X_2 and X_3 form neither a right-handed nor a left-handed co-ordinate system, and are different from axes x_1^p , x_2^p and x_3^p used by Wong and Trifunac¹⁹ ($X_1 = x_1^p$, $X_2 = x_2^p$, $X_3 = -x_3^p$). Also, the direction of angles α_1 , α_2 , and α_3 is different. (If α_i^p 's are the angles in their paper, then $\alpha_1 = -\alpha_1^p$, $\alpha_2 = -\alpha_2^p$ and $\alpha_3 = \alpha_3^p$). Axes X_1 , X_2 and X_3 are, orientated so that the dynamic equilibrium equations for all the three penduli, for small deflections, have the

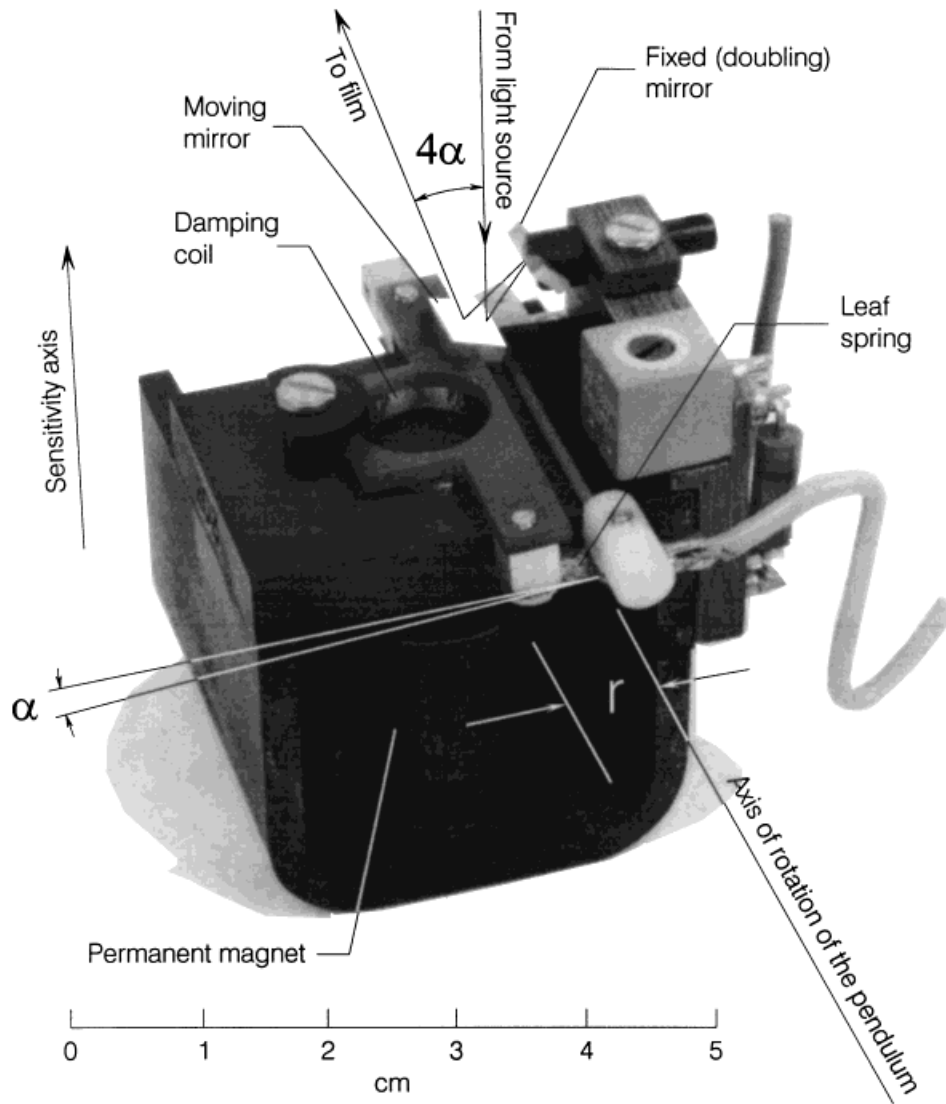


Figure 2. An SMA-1 transducer removed from the box. Letter r symbolically indicates the arm of the pendulum and α is the angle of deflection. Double reflection of the light beam from the mirror attached to the pendulum creates rotation of the light beam by angle 4α

standard form.²³ The V transducer (Pendulum 3) is different from the other two in that it is affected by gravity. 'Horizontal' pendulum, or $\alpha_3 = 0$, corresponds to the static equilibrium position under the action of gravity.

Figure 5 shows the mathematical model of the i th pendulum (mass m_i , arm is r_i , spiral stiffness K_i and spiral damping C_i). The pivot axis is perpendicular to the plane of the paper. For small α_i , the transducer is sensitive only to forces or accelerations along the X_i -axis. A force f_i , or support acceleration \ddot{X}_i , are defined as positive if pointing in the positive X_i -direction. The force, f_i , is shown in brackets. The dynamic balance of moments about the pivot axis through O implies

$$m_i r_i^2 \ddot{\alpha}_i + C_i \dot{\alpha}_i + K_i \alpha_i = -m_i \ddot{X}_i r_i \quad (2)$$

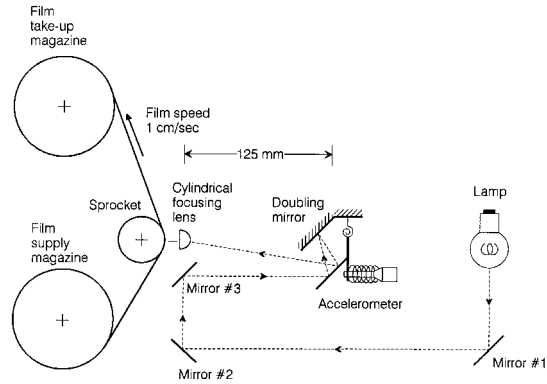


Figure 3. Schematic representation of the optical path in an SMA-1 accelerograph. The film transport, light path and cylindrical lens are shown as viewed along the transverse (T) axis (see Figure 1). The longitudinal (L) accelerometer and doubling mirror are shown as viewed from the vertical (V) axis. The transverse (T) and vertical (V) transducers have additional 90° mirrors (not shown) receiving light from mirror no. 3, and reflecting it again, after it was deflected by the transducer mirrors, towards the cylindrical focussing lens in front of the film

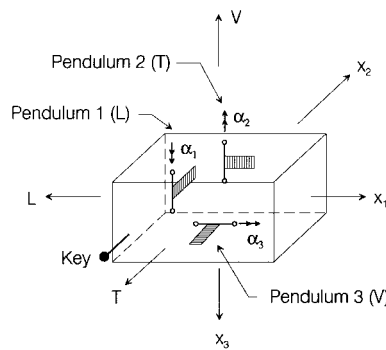


Figure 4. Schematic representation of the three transducers in an SMA-1 accelerograph, all in 'normal' position. Symbols L , V and T indicate the directions of the sensitivity axes. Axes X_1 , X_2 and X_3 are used to describe the motion. Angles α_1 , α_2 and α_3 measure the deflection of the L-, T- and V-transducer, respectively

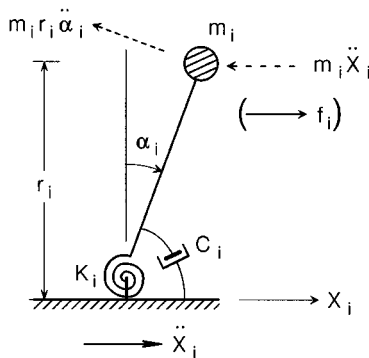


Figure 5. Mathematical model of the transducer—a physical pendulum of length r_i , mass m_i , stiffness K_i and damping C_i . For small deflections α_i , the pendulum is sensitive only to forces or accelerations along the X_i -axis

Introducing circular frequency ω_i , damping ratio, ζ_i , and angular sensitivity constant, s_i^α , such that

$$\omega_i^2 = K_i / (m_i r_i^2) \quad (3)$$

$$2\omega_i \zeta_i = C_i / (m_i r_i^2) \quad (4)$$

and

$$s_i^\alpha = \frac{1}{\omega_i^2 r_i} \quad (5)$$

equation (2) results in

$$\ddot{\alpha}_i + 2\omega_i \zeta_i \dot{\alpha}_i + \omega_i^2 \alpha_i = -\omega_i^2 s_i^\alpha \ddot{X}_i \quad (6)$$

The constants m_i , K_i , C_i and r_i are difficult to measure, but ω_i , ζ_i , and s_i^α can be measured easily.³

The natural frequency of the transducer (~ 25 Hz) is higher than most frequencies carrying the major portion of energy in strong ground motion. Then, $\omega_i^2 \alpha_i$ is larger than the other two terms in the LHS of equation (6), which implies

$$\alpha_i \approx -s_i^\alpha \ddot{X}_i \quad (7)$$

Equation (7) shows that the response, α_i , is approximately proportional to support acceleration in the $-X_i$ direction, i.e. in positive L , T or V directions.

The angular sensitivity s_i^α equals the angle of deflection caused by unit acceleration and is in units $\text{rad} \times \text{s}^2/\text{m}$. The inverse of s_i^α is the angular amplification constant

$$a_i^\alpha = \frac{1}{s_i^\alpha} \quad (8)$$

in units $\text{m}/(\text{rad} \times \text{s}^2)$. The amplification equals the ground acceleration that results in 1 rad deflection of the pendulum. It has been customary to use g as unit of acceleration, which leads to sensitivity and amplification constants, $s_i^{\alpha,w}$ and $a_i^{\alpha,w}$, in units rad/g and g/rad . The relationship between s_i^α and $s_i^{\alpha,w}$ is

$$s_i^{\alpha,w} = s_i^\alpha g \quad (9)$$

and $a_i^{\alpha,w}$ is the inverse of $s_i^{\alpha,w}$. The sensitivity of accelerographs recording on film is usually evaluated directly from trace deflection on the film, y_i , and is expressed in units cm/g . If sensitivity s_i^y is the trace deflection y_i when $1g$ acceleration is measured, and if in neutral position the light beam is perpendicular to the film, from equation (1), it follows that

$$s_i^y = d \tan(4s_i^\alpha) \quad (10)$$

The angular sensitivity s_i^α is a constant, specific for each transducer. If there are no obstacles, k times larger acceleration along the sensitivity axis would result in k times larger angle of deflection, α_i , but not in k times larger deflection on the film, y_i , as y_i is not a linear function of α_i . Therefore, the sensitivity s_i^y is a function of the acceleration, and equation (10) gives the value for acceleration $1g$. This implies that errors are introduced if the deflection on the film, y_i , is scaled directly to acceleration units by constant sensitivity, s_i^y . An analysis of these errors is presented in References 21 and 22.

Equations of motion for large deflections and misaligned transducers

Co-ordinate axes X_1 , X_2 and X_3 (Figure 4) are perpendicular to each other, and if the transducers are perfectly aligned to these axes, for small deflections, three orthogonal components of motion are recorded. However, the actual position of each pendulum is, in general, slightly off this ideal position. Three auxiliary co-ordinate systems can be introduced, with respect to which the penduli are perfectly aligned and transformations

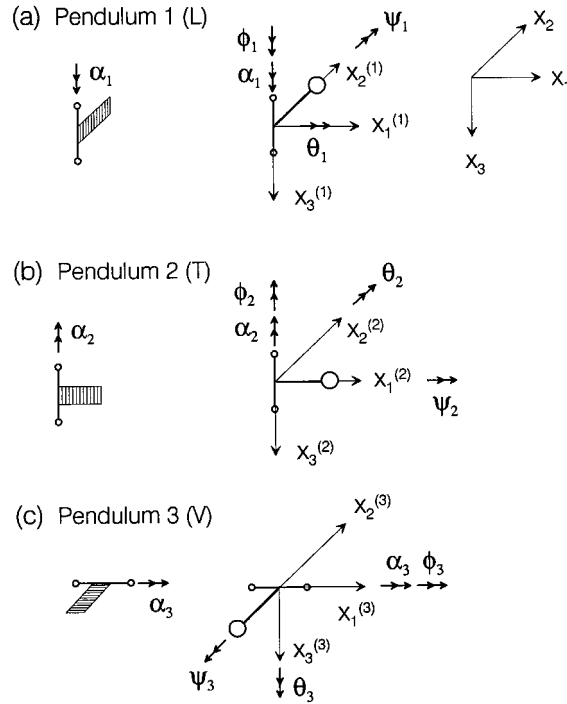


Figure 6. Misalignment angles for the three penduli (ϕ_i, ψ_i and $\theta_i, i = 1, 2$ and 3), shown by double arrows

defining the position of the auxiliary systems, with respect to the orthogonal $X_1-X_2-X_3$ system. Then, the equations of motion can be transformed to the $X_1-X_2-X_3$ system, and relationships between the unknown components of motion in the $X_1-X_2-X_3$ co-ordinate system and the angles of deflection $\alpha_i, i = 1, 2$ and 3 can be established.

(a) *Auxiliary co-ordinate systems and transformations.* The auxiliary co-ordinate system for the i th pendulum is $X_1^{(i)}-X_2^{(i)}-X_3^{(i)}$. Axes $X_1^{(i)}, X_2^{(i)}$ and $X_3^{(i)}$ point approximately in same direction as axes X_1, X_2 and X_3 , but are slightly off. The alignment of the penduli with respect to these co-ordinate systems is shown in Figure 6. Axes $X_i^{(i)}, i = 1, 2, 3$ are aligned with the sensitivity axes.

The position of the i th auxiliary system can be obtained by consecutive rotation of the system $X_1-X_2-X_3$ through small angles ϕ_i, θ_i and ψ_i (shown in Figure 6 by vectors) such that

$\phi_i =$ rotation about the ideal position of the pivot axis;

$\theta_i =$ rotation of the ideal pivot axis about the ideal sensitivity axis;

$\psi_i =$ rotation of the ideal pivot axis about the axis aligned with the ideal position of the arm of the pendulum.

Let $[T^{(i)}], i = 1, 2, 3$ be transformation matrices that would bring the $X_1-X_2-X_3$ system parallel to the corresponding auxiliary systems (these are products of the corresponding rotation matrices). Then

$$\begin{Bmatrix} X_1^{(i)} \\ X_2^{(i)} \\ X_3^{(i)} \end{Bmatrix} = [T^{(i)}] \begin{Bmatrix} X_1 \\ X_2 \\ X_3 \end{Bmatrix} \tag{11}$$

Matrices $[T^{(i)}]$ are same as those in Reference 19, subject to the appropriate transformation of the co-ordinate axes and angles. For the configuration used in this paper, these matrices can be found in Reference 21.

(b) *Equations of motion for large deflections in the aligned reference systems.* Due to orthogonality of the auxiliary reference systems and alignment, each pendulum is sensitive only to motion in a plane defined by two of the co-ordinate axes. These planes are $X_1^{(1)}-X_2^{(1)}$ for Pendulum 1, $X_1^{(2)}-X_2^{(2)}$ for Pendulum 2, and $X_2^{(3)}-X_3^{(3)}$ for Pendulum 3. Free-body diagrams of the penduli are shown in Figure 7. Dynamic equilibrium of moments about axes $X_3^{(1)}$, $X_3^{(2)}$ and $X_1^{(3)}$ implies

$$m_1 r_1^2 \ddot{\alpha}_1 + m_1 (r_1 \cos \alpha_1) \ddot{X}_1^{(1)} - m_1 (r_1 \sin \alpha_1) \ddot{X}_2^{(1)} + C_1 \dot{\alpha}_1 + K_1 \alpha_1 = 0 \tag{12a}$$

$$m_1 r_2^2 \ddot{\alpha}_2 - m_2 (r_2 \sin \alpha_2) \ddot{X}_1^{(2)} + m_2 (r_2 \cos \alpha_2) \ddot{X}_2^{(2)} + C_2 \dot{\alpha}_2 + K_2 \alpha_2 = 0 \tag{12b}$$

$$m_3 r_3^2 \ddot{\alpha}_3 + m_3 (r_3 \cos \alpha_3) \ddot{X}_3^{(3)} + m_3 (r_3 \sin \alpha_3) \ddot{X}_2^{(3)} + C_3 \dot{\alpha}_3 + K_3 \alpha_3 = 0 \tag{12c}$$

and

$$\cos \alpha_1 \ddot{X}_1^{(1)} - \sin \alpha_1 \ddot{X}_2^{(1)} = r_1 (\ddot{\alpha}_1 + 2\omega_1 \zeta_1 \dot{\alpha}_1 + \omega_1^2 \alpha_1) \tag{13a}$$

$$\sin \alpha_2 \ddot{X}_1^{(2)} + \cos \alpha_2 \ddot{X}_2^{(2)} = r_2 (\ddot{\alpha}_2 + 2\omega_2 \zeta_2 \dot{\alpha}_2 + \omega_2^2 \alpha_2) \tag{13b}$$

$$\sin \alpha_3 \ddot{X}_2^{(3)} + \cos \alpha_3 \ddot{X}_3^{(3)} = r_3 (\ddot{\alpha}_3 + 2\omega_3 \zeta_3 \dot{\alpha}_3 + \omega_3^2 \alpha_3) \tag{13c}$$

The above equations relate the measurable transducer responses α_i , $i = 1, 2$ and 3 to components of motion along the axes of the auxiliary systems.

(c) *Equations of motion for large deflections, in the non-aligned system.* From equation (11), it follows that the accelerations in the auxiliary reference systems and in the system $X_1-X_2-X_3$ are related by

$$\begin{Bmatrix} \ddot{X}_1^{(i)} \\ \ddot{X}_2^{(i)} \\ \ddot{X}_3^{(i)} \end{Bmatrix} = [T^{(i)}] \begin{Bmatrix} \ddot{X}_1 \\ \ddot{X}_2 \\ \ddot{X}_3 \end{Bmatrix}, \quad i = 1, 2, 3 \tag{14}$$

The equations of motion in the $X_1-X_2-X_3$ system can be obtained by substituting $\{\ddot{X}_1^{(i)}, \ddot{X}_2^{(i)}, \ddot{X}_3^{(i)}\}^T$ in equations (13) from equation (14). This leads to the system of equations

$$[T] \begin{Bmatrix} \ddot{X}_1 \\ \ddot{X}_2 \\ \ddot{X}_3 \end{Bmatrix} = \{b\} \tag{15}$$

where

$$[T] = \begin{bmatrix} \cos \alpha_1 T_{11}^{(1)} & \cos \alpha_1 T_{12}^{(1)} & \cos \alpha_1 T_{13}^{(1)} \\ -\sin \alpha_1 T_{21}^{(1)} & -\sin \alpha_1 T_{22}^{(1)} & -\sin \alpha_1 T_{23}^{(1)} \\ \sin \alpha_2 T_{11}^{(2)} & -\sin \alpha_2 T_{12}^{(2)} & -\sin \alpha_2 T_{13}^{(2)} \\ +\cos \alpha_2 T_{21}^{(2)} & +\cos \alpha_2 T_{22}^{(1)} & +\cos \alpha_2 T_{23}^{(2)} \\ \sin \alpha_3 T_{21}^{(3)} & \sin \alpha_3 T_{22}^{(3)} & \sin \alpha_3 T_{23}^{(3)} \\ +\cos \alpha_3 T_{31}^{(3)} & +\cos \alpha_3 T_{32}^{(3)} & +\cos \alpha_3 T_{33}^{(3)} \end{bmatrix} \tag{16}$$

and

$$\{b\} = \begin{Bmatrix} -r_1 (\ddot{\alpha}_1 + 2\omega_1 \zeta_1 \dot{\alpha}_1 + \omega_1^2 \alpha_1) \\ -r_2 (\ddot{\alpha}_2 + 2\omega_2 \zeta_2 \dot{\alpha}_2 + \omega_2^2 \alpha_2) \\ -r_3 (\ddot{\alpha}_3 + 2\omega_3 \zeta_3 \dot{\alpha}_3 + \omega_3^2 \alpha_3) \end{Bmatrix} \tag{17}$$

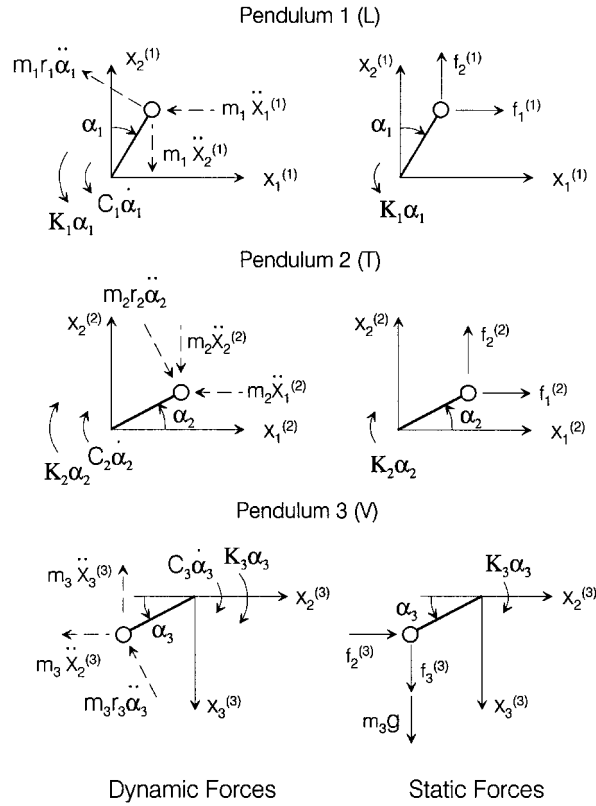


Figure 7. Free-body diagrams of the penduli in the auxiliary reference systems, under action of static or dynamic forces

$(T_{lk}^{(i)})$ are terms of matrices $[T^{(i)}]$. The misalignment angles are usually small (of the order of few degrees). Angles α_i are also small which implies

$$[T] = \begin{bmatrix} 1 & -\varphi_1 - \alpha_1 & \psi_1 \\ -\alpha_2 - \varphi_2 & 1 & -\psi_2 \\ \psi_3 & \alpha_3 + \varphi_3 & 1 \end{bmatrix} + O(\varphi_i^2, \psi_i^2, \theta_i^2, \alpha_i^2) \tag{18}$$

The linearized $[T]$ does not depend on misalignment angles θ_i .

Response to static forces

Static forces, defined in the X_1 - X_2 - X_3 reference system can be transformed to the auxiliary systems by

$$\begin{Bmatrix} f_1^{(i)} \\ f_2^{(i)} \\ f_3^{(i)} \end{Bmatrix} = [T^{(i)}] \begin{Bmatrix} f_1 \\ f_2 \\ f_3 \end{Bmatrix} \tag{19}$$

where f_1, f_2 and f_3 are force components in the X_1 - X_2 - X_3 reference system, and $f_1^{(i)}, f_2^{(i)}$ and $f_3^{(i)}$ in the $X_1^{(i)} - X_2^{(i)} - X_3^{(i)}$ reference systems. Then the static equilibrium equations can be written with respect to the

aligned system. The free-body diagrams in Figure 7 imply

$$K_1\alpha_1 + f_2^{(1)}r_1 \sin \alpha_1 - f_1^{(1)}r_1 \cos \alpha_1 = 0 \quad (20a)$$

$$K_2\alpha_2 + f_1^{(2)}r_2 \sin \alpha_2 - f_2^{(2)}r_2 \cos \alpha_2 = 0 \quad (20b)$$

$$K_3(\alpha_3 + \alpha_3^0) - f_3^{(3)}r_3 \cos \alpha_3 - f_2^{(3)}r_3 \sin \alpha_3 = 0 \quad (20c)$$

where α_3^0 is the deflection of the V-pendulum caused by its weight, m_3g , applied in the positive $X_3^{(3)}$ direction. In the normal position, when the pendulum is ideally horizontal (the arm of the pendulum is perpendicular to the $X_3^{(3)}$ -axis), $\alpha_3 = 0$, but the spring is stretched to an angle α_3^0 equal to

$$\alpha_3^0 = s_3^{\alpha,w} \quad (21)$$

In terms of the sensitivity constants $s_i^{\alpha,w}$, equations (20) appear as

$$\cos \alpha_1 f_1^{(1)} - \sin \alpha_1 f_2^{(1)} = \alpha_1(m_1g)/s_1^{\alpha,w} \quad (22a)$$

$$-\sin \alpha_2 f_1^{(2)} + \cos \alpha_2 f_2^{(2)} = \alpha_2(m_2g)/s_2^{\alpha,w} \quad (22b)$$

$$\sin \alpha_3 f_2^{(3)} + \cos \alpha_3 f_3^{(3)} = (\alpha_3 + \alpha_3^0)(m_3g)/s_3^{\alpha,w} \quad (22c)$$

Then, for small deflections the sensitivity $s_i^{\alpha,w}$ equals the deflection of the pendulum, α_i , when force equal to its weight is applied along the sensitivity axis.

From equations (19) and (22), the equilibrium equations can be written in the X_1 - X_2 - X_3 system

$$[T] \begin{Bmatrix} f_1 \\ f_2 \\ f_3 \end{Bmatrix} = \begin{Bmatrix} \alpha_1(m_1g)a_1^{\alpha,w} \\ \alpha_2(m_2g)a_2^{\alpha,w} \\ (\alpha_3 + \alpha_3^0)(m_3g)a_3^{\alpha,w} \end{Bmatrix} \quad (23)$$

THE INVERSE PROBLEM

The misalignment angles and the sensitivity constants can be determined from equations (23) if the static forces f_i and the deflection angles α_i are known. The static tilt test described by Wong and Trifunac¹⁹ can be used to obtain a series of independent measurements. The instrument is rotated through accurately measured angles and trace deflections, y_i , are recorded on the film. The static force is a fraction of the pendulum weight, and is determined from the angle of rotation. The trace deflections y_i are measured by scanning the film with 300 or 600 points/in resolution (1 in = 2.54 cm) and digitizing the scanned image by a computer. The angles α_i are then calculated using equation (1), or by another more accurate procedure, proposed by Todorovska et al.,^{21,22} which corrects also for inclined ray incidence onto the film. Each instrument position leads to one equation per pendulum. Finally, three independent systems of equations are obtained. The following presents an algorithm for solution.

Static tilt test

For each instrument position, static equilibrium is defined by equations (23). For stable numerical inversion, the linearized form of $[T]$ in equation (18) may be used. Then there are only three unknowns, φ_i , ψ_i and the amplification $a_i^{\alpha,w}$. Minimum three linearly independent equations per pendulum are required. However, it is better to perform additional measurements, because of possible errors or missing data (e.g., for large deflections, the pendulum motion may be limited by an obstacle, or the trace may go off the film). All errors may not be obvious from visual film inspection, and it is best if an overdetermined system of equations is solved by least squares. Unusually large residuals will indicate that a measurement may be 'corrupted'. The problem is then fixed, or the corresponding equation is disregarded, and the system is solved again.

Controlled tilting is performed by the table shown in Figure 8. The instrument is securely attached to a base plate, which can be rotated about its vertical axis of symmetry (counterclockwise, up to 90°) and about

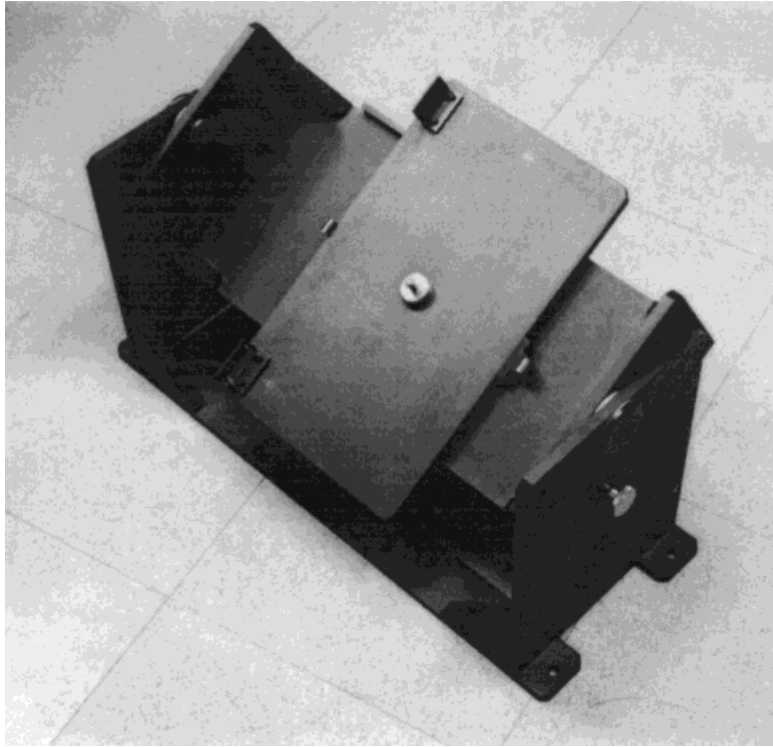


Figure 8. Tilt table rotated by 30° about its longitudinal axis, and with the instrument plate rotated counterclockwise through 90° . This position corresponds to the step of the tilt test in which the SMA-1 is rotated about its transverse axis through 30° , with the key in lower position

its long axis. Rotation of the base plate about the transverse axis is possible by first rotating it through 90° horizontally, and then rotating by the desired angle about the long axis of the table. Figure 8 shows the base plate rotated through 30° about the transverse axis.

The sequence of steps in a tilt test is shown on the field form which is reproduced in Figure 9. The positions are identified by letters (A through I and B' through I'). In each position, the instrument records for about 2 s. Figure 10 shows the film, and Figure 11 a sketch of realistic trace deflections (the traces have been shifted to avoid intermingling).

The tilt table in Figure 8 is different from the one used by Wong and Trifunac¹⁹ in that no adjustment is possible to make it horizontal. In field conditions, the table can easily be off horizontal by few degrees, which is of the same order of magnitude as the misalignment angles. The algorithm presented in this paper takes this into account. Two angles, describing the position of the tilt table angles, are treated as unknowns and are evaluated by the presented algorithm for processing the tilt test measurements. One might be tempted to construct a tilt table with three adjustable legs and an accurate levelling mechanism. In rough field conditions, this would require additional work and time. However, even with perfectly horizontal tilt table, the ideal reference systems for the three transducers would still not be perfectly horizontal, because of manufacturing tolerances and not so precise placement of the transducers into the instrument housing. The presented algorithm, besides simplifying the field work, also accounts for these imperfections which are not possible to measure directly. The unknown 'tilt table angles', in fact, are combination of these imperfections and the directly measurable angles of the tilt table. In what follows, the inverse problem is first presented for a perfectly horizontal tilt table, and then for a tilt table that is off horizontal.

TILT TEST PROCEDURE

1. Thread film. Attach cover.
2. Attach SMA-1 to tilt table.
3. Insert connector with switch into plug.
4. Run the following records in exactly this order.
 - A. Normal Operating Position. Use KEY.
 - TEST (2 sec)
 - CAL (2 sec)
 - NAT FREQ (2 sec)
 - CAL (2 sec)
 - TEST (2 sec)
 - B. Rotated 90° about long. axis. Key side down. Switch (1 sec)
 - C. Upside down
 - D. Rotated 90° about long. axis. Key side up.
 - E. Normal position.
 - F. Rotate base plate - normal position.
 - G. Rotate 90° about transverse axis. Key up in air.
 - H. Rotate 90° about transverse axis. Key in lower position.
 - I. Normal position (base plate rotated).
5. Repeat steps 4B, D-I. But this time all rotations are 30° from horizontal
 - B'. Rotated 30° about long. axis. Key side down. Switch (1 sec)
 - C'. Skip.
 - D'. Rotated 30° about long. axis. Key side up.
 - E'. Normal position.
 - F'. Rotate base plate - normal position.
 - G'. Rotate 30° about transverse axis. Key up in air.
 - H'. Rotate 30° about transverse axis. Key in lower position.
 - I'. Normal position (base plate rotated).
6. TEST (2 sec)
CAL (2 sec)
NAT FREQ (2 sec)
CAL (2 sec)
TEST (2 sec)
OFF.
7. Remove film: Scratch in serial number.
8. Process film.

Date:
S/N:
Station:
Place of the test:

Operators:

Figure 9. A standard form to be filled out during a tilts test

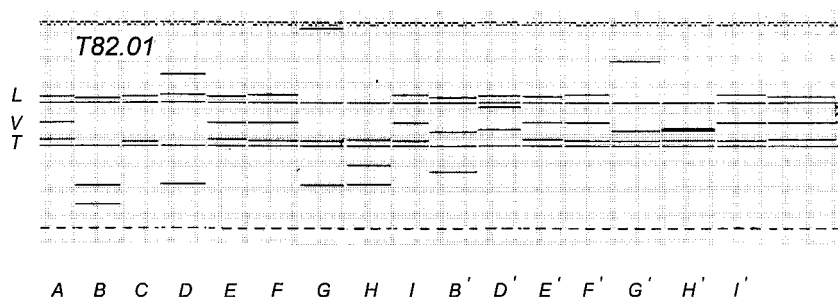


Figure 10. Film with tilt test T82-01

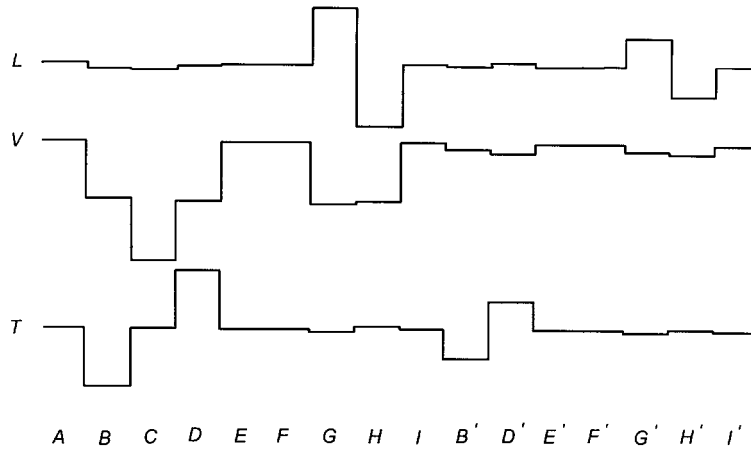


Figure 11. A schematic representation of the trace deflections for the standard sequence of instrument positions (see Figures 8 and 9). For clarity, the traces have been shifted vertically relative to each other

Equilibrium equation for a perfectly horizontal tilt table

The mass of each pendulum is different, and the static forces for a given tilt table position are different. However, the force normalized by the weight

$$\mathbf{F}_n = \{f_1, f_2, f_3\}^T / (m_i g) \tag{24}$$

is the same for all penduli. For perfectly horizontal tilt table, the normalized forces for positions *A* through *I* and *B'* through *I'* are:

$$L: \mathbf{F}_n^A = \{0, 0, 1\}^T \tag{25a}$$

$$L: \mathbf{F}_n^B = \{0, -1, 0\}^T \tag{25b}$$

$$L: \mathbf{F}_n^C = \{0, 0, -1\}^T \tag{25c}$$

$$L: \mathbf{F}_n^D = \{0, 1, 0\}^T \tag{25d}$$

$$L: \mathbf{F}_n^E = \{0, 0, 1\}^T \tag{25e}$$

$$T: \mathbf{F}_n^F = \{0, 0, 1\}^T \tag{25f}$$

$$T: \mathbf{F}_n^G = \{1, 0, 0\}^T \tag{25g}$$

$$T: \mathbf{F}_n^H = \{-1, 0, 0\}^T \tag{25h}$$

$$T: \mathbf{F}_n^I = \{0, 0, 1\}^T \tag{25i}$$

$$L: \mathbf{F}_n^{B'} = \{0, -\sin 30^\circ, \cos 30^\circ\}^T \tag{25j}$$

$$L: \mathbf{F}_n^{D'} = \{0, \sin 30^\circ, \cos 30^\circ\}^T \tag{25k}$$

$$L: \mathbf{F}_n^{E'} = \{0, 0, 1\}^T \tag{25l}$$

$$T: \mathbf{F}_n^{F'} = \{0, 0, 1\}^T \tag{25m}$$

$$T: \mathbf{F}_n^{G'} = \{\sin 30^\circ, 0, \cos 30^\circ\}^T \tag{25n}$$

$$T: \mathbf{F}_n^{H'} = \{-\sin 30^\circ, 0, \cos 30^\circ\}^T \tag{25o}$$

$$T: \mathbf{F}_n^{I'} = \{0, 0, 1\}^T \tag{25p}$$

L and T to the left of the above equations indicate rotation (or the corresponding ‘normal’ position) about the longitudinal or the transverse axes of the instrument. The superscripts indicate the instrument position. The same superscript can be attached to the corresponding angles of deflection α_i . For each position, and each pendulum one equilibrium equation is obtained, by substituting the corresponding force and angle in equations (23). Positions E and E' and F and F' will be ignored as redundant (E and E' are same as A , and F and F' are same as I).

Since the normalized force is same for the three penduli, the equilibrium equations (23) for a particular position can be written as

$$\begin{bmatrix} 1 & -\varphi_1 - \alpha_1 & \psi_1 \\ -\alpha_2 - \varphi_2 & 1 & -\psi_2 \\ \psi_3 & \alpha_3 + \varphi_3 & 1 \end{bmatrix} \mathbf{F}_n = \begin{Bmatrix} \alpha_1 a_1^{z,w} \\ \alpha_2 a_2^{z,w} \\ (\alpha_3 + \alpha_3^0) a_3^{z,w} \end{Bmatrix} \quad (26)$$

The constants $a_i^{z,w}$ represent the amplification.

Equilibrium equation for a nonhorizontal tilt table

The tilt table is, in general, off horizontal by angles δ_1 and δ_2 representing rotation about the longer and the shorter axes of the table, as shown in Figure 12. Parts (a) and (b) correspond to the instrument in normal position and in normal position-base plate rotated (Figure 9). The ‘key’ schematically indicates the instrument orientation (Figure 1). The misalignment angles are also indicated. In the first-order approximation, the effect of the angles δ_1 and δ_2 just adds to the effects of the misalignment angles. So, one can assume that the same equilibrium equations hold as for the case when the table is horizontal, but the misalignment angles are modified (the modification is different for the ‘normal’ (L) and for the ‘normal-base-plate rotated’ (T) positions). The ‘effective’ misalignment angles can be determined from Figure 12, and then ‘effective’ transformation matrices $[T_L^{\text{eff}}]$ and $[T_T^{\text{eff}}]$ can be constructed for tilting about the longitudinal and transverse axis, respectively. These matrices are

$$[T_L^{\text{eff}}] = \begin{bmatrix} 1 & -\varphi_1 - \alpha_1 & (\psi_1 + \delta_2) \\ -\alpha_2 - \varphi_2 & 1 & -(\psi_2 + \delta_1) \\ (\psi_3 - \delta_2) & \alpha_3 + (\varphi_3 + \delta_1) & 1 \end{bmatrix} \quad (27a)$$

and

$$[T_T^{\text{eff}}] = \begin{bmatrix} 1 & -\varphi_1 - \alpha_1 & (\psi_1 - \delta_1) \\ -\alpha_2 - \varphi_2 & 1 & -(\psi_2 + \delta_2) \\ (\psi_3 + \delta_1) & \alpha_3 + (\varphi_3 + \delta_2) & 1 \end{bmatrix} \quad (27b)$$

and the new equilibrium equations are

$$L: [T_L^{\text{eff}}] \mathbf{F}_n = \begin{Bmatrix} \alpha_1 a_1^{z,w} \\ \alpha_2 a_2^{z,w} \\ (\alpha_3 + \alpha_3^0) a_3^{z,w} \end{Bmatrix} \quad (28a)$$

$$T: [T_T^{\text{eff}}] \mathbf{F}_n = \begin{Bmatrix} \alpha_1 a_1^{z,w} \\ \alpha_2 a_2^{z,w} \\ (\alpha_3 + \alpha_3^0) a_3^{z,w} \end{Bmatrix} \quad (28b)$$

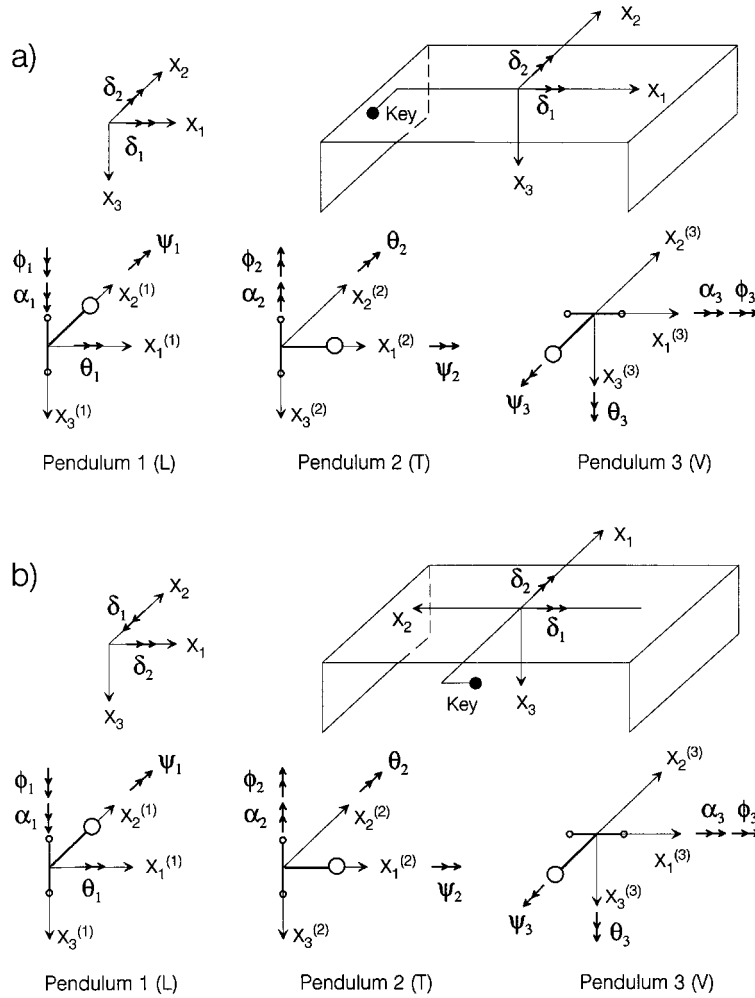


Figure 12. A schematic representation of the tilt table and angles δ_1 and δ_2 describing by how much the table is off vertical. Axes X_1 , X_2 and X_3 , which are aligned to the instrument box, and the misalignment angles are also shown for (a) the 'normal position' and (b) the 'normal position—base plate rotated'

Matrices $[T_L^{eff}]$ and $[T_T^{eff}]$ can be represented as a sum of the identity matrix and matrices $[T_{\varphi,\psi}]$, $[T_\alpha]$ and $[T_\delta]$ as follows:

$$[T_L^{eff}] = [I] + [T_{\varphi,\psi}] + [T_\alpha] + [T_{\delta,L}] \tag{29a}$$

and

$$[T_T^{eff}] = [I] + [T_{\varphi,\psi}] + [T_\alpha] + [T_{\delta,T}] \tag{29b}$$

where

$$[T_{\varphi,\psi}] = \begin{bmatrix} 0 & -\varphi_1 & \psi_1 \\ -\varphi_2 & 0 & -\psi_2 \\ \psi_3 & \varphi_3 & 0 \end{bmatrix} \tag{30}$$

$$[T_\alpha] = \begin{bmatrix} 0 & -\alpha_1 & 0 \\ -\alpha_2 & 0 & 0 \\ 0 & \alpha_3 & 0 \end{bmatrix} \quad (31)$$

$$[T_{\delta,L}] = \begin{bmatrix} 0 & 0 & \delta_2 \\ 0 & 0 & -\delta_1 \\ -\delta_2 & \delta_1 & 0 \end{bmatrix} \quad (32a)$$

and

$$[T_{\delta,T}] = \begin{bmatrix} 0 & 0 & -\delta_1 \\ 0 & 0 & -\delta_2 \\ \delta_1 & \delta_2 & 0 \end{bmatrix} \quad (32b)$$

Difference equations with respect to normal positions

If there is no misalignment and the table is horizontal, the traces on the film for the normal position, or normal position-base plate rotated, would correspond to $\alpha_i = 0$. In general, this is not the case, and the trace positions corresponding to $\alpha_i = 0$ are not known. However, the distance between the traces for different instrument positions and the corresponding differences in angles α can be determined. Positions *A* and *I* can be used as reference for tilting about the longitudinal and the transverse axes, respectively. From the eleven nontrivial equilibrium equations, nine difference equations can be constructed:

$$L, (1): B - A$$

$$L, (2): C - A$$

$$L, (3): D - A$$

$$T, (4): G - I$$

$$T, (5): H - I$$

$$L, (6): B' - A$$

$$L, (7): D' - A$$

$$T, (8): G' - I$$

$$T, (9): H' - I$$

The deflection angles α_i appear on both sides of the equilibrium equations. Therefore, in the difference equations, the absolute angles α_i cannot be replaced throughout by the differences of angles.

We first define relative normalized forces

$$L: \mathbf{F}_n^r = \mathbf{F}_n - \mathbf{F}_n^A \quad (33a)$$

$$T: \mathbf{F}_n^r = \mathbf{F}_n - \mathbf{F}_n^I \quad (33b)$$

and relative angles

$$L: \alpha_i^r = \alpha_i - \alpha_i^A \quad (34a)$$

$$T: \alpha_i^r = \alpha_i - \alpha_i^I \quad (34b)$$

Then the difference equations can be written as follows:

$$L: [[T_{\varphi,\psi}] + [T_{\alpha^A}]]\mathbf{F}_n^r - \{a_i^{z,w}\alpha_i^r\} = [[I] + [T_{\alpha^r}]]\mathbf{F}_n^r - [T_{\delta,L}]\mathbf{F}_n^r \quad (35a)$$

and

$$T: [[T_{\varphi,\psi}] + [T_{\alpha'}]]\mathbf{F}_n^r - \{a_i^{z,w} \alpha_i^r\} = [[I] + [T_{\alpha'}]]\mathbf{F}_n^r - [T_{\delta,T}]\mathbf{F}_n^r \tag{35b}$$

resulting in the following three systems of equations for Penduli 1, 2 and 3:

$$\begin{bmatrix} 1 & -1 & -\alpha_1^{(1)} \\ 0 & -2 & -\alpha_1^{(2)} \\ -1 & -1 & -\alpha_1^{(3)} \\ 0 & -1 & -\alpha_1^{(4)} \\ 0 & -1 & -\alpha_1^{(5)} \\ \frac{1}{2} & \frac{\sqrt{3}}{2} - 1 & -\alpha_1^{(6)} \\ -\frac{1}{2} & \frac{\sqrt{3}}{2} - 1 & -\alpha_1^{(7)} \\ 0 & \frac{\sqrt{3}}{2} - 1 & -\alpha_1^{(8)} \\ 0 & \frac{\sqrt{3}}{2} - 1 & -\alpha_1^{(9)} \end{bmatrix} \begin{Bmatrix} \varphi_1^* \\ \psi_1 \\ a_1^{z,w} \end{Bmatrix} = \begin{Bmatrix} -\alpha_1^{(1)} \\ 0 \\ \alpha_1^{(3)} \\ -1 \\ 1 \\ -\frac{1}{2}\alpha_1^{(6)} \\ \frac{1}{2}\alpha_1^{(7)} \\ -\frac{1}{2} \\ \frac{1}{2} \end{Bmatrix} - \begin{Bmatrix} -\delta_2 \\ -2\delta_2 \\ -\delta_2 \\ \delta_1 \\ \delta_1 \\ \delta_2(\frac{\sqrt{3}}{2} - 1) \\ \delta_2(\frac{\sqrt{3}}{2} - 1) \\ -\delta_1(\frac{\sqrt{3}}{2} - 1) \\ -\delta_1(\frac{\sqrt{3}}{2} - 1) \end{Bmatrix} \tag{36a}$$

$$\begin{bmatrix} 0 & 1 & -\alpha_2^{(1)} \\ 0 & 2 & -\alpha_2^{(2)} \\ 0 & 1 & -\alpha_2^{(3)} \\ -1 & 1 & -\alpha_2^{(4)} \\ 1 & 1 & -\alpha_2^{(5)} \\ 0 & -(\frac{\sqrt{3}}{2} - 1) & -\alpha_2^{(6)} \\ 0 & -(\frac{\sqrt{3}}{2} - 1) & -\alpha_2^{(7)} \\ -\frac{1}{2} & -(\frac{\sqrt{3}}{2} - 1) & -\alpha_2^{(8)} \\ \frac{1}{2} & -(\frac{\sqrt{3}}{2} - 1) & -\alpha_2^{(9)} \end{bmatrix} \begin{Bmatrix} \varphi_2^* \\ \psi_2 \\ a_2^{z,w} \end{Bmatrix} = \begin{Bmatrix} 1 \\ 0 \\ -1 \\ \alpha_2^{(4)} \\ -\alpha_2^{(5)} \\ \frac{1}{2} \\ -\frac{1}{2} \\ \frac{1}{2}\alpha_2^{(8)} \\ -\frac{1}{2}\alpha_2^{(9)} \end{Bmatrix} - \begin{Bmatrix} \delta_1 \\ 2\delta_1 \\ \delta_1 \\ \delta_2 \\ \delta_2 \\ -\delta_1(\frac{\sqrt{3}}{2} - 1) \\ -\delta_1(\frac{\sqrt{3}}{2} - 1) \\ -\delta_2(\frac{\sqrt{3}}{2} - 1) \\ -\delta_2(\frac{\sqrt{3}}{2} - 1) \end{Bmatrix} \tag{36b}$$

and

$$\begin{bmatrix} -1 & 0 & -\alpha_3^{(1)} \\ 0 & 0 & -\alpha_3^{(2)} \\ 1 & 0 & -\alpha_3^{(3)} \\ 0 & 1 & -\alpha_3^{(4)} \\ 0 & -1 & -\alpha_3^{(5)} \\ -\frac{1}{2} & 0 & -\alpha_3^{(6)} \\ \frac{1}{2} & 0 & -\alpha_3^{(7)} \\ 0 & \frac{1}{2} & -\alpha_3^{(8)} \\ 0 & -\frac{1}{2} & -\alpha_3^{(9)} \end{bmatrix} \begin{Bmatrix} \varphi_3^* \\ \psi_3 \\ a_3^{z,w} \end{Bmatrix} = \begin{Bmatrix} \alpha_3^{(1)} + 1 \\ 2 \\ -\alpha_3^{(2)} + 1 \\ 1 \\ 1 \\ \frac{1}{2}\alpha_3^{(6)} - (\frac{\sqrt{3}}{2} - 1) \\ -\frac{1}{2}\alpha_3^{(7)} - (\frac{\sqrt{3}}{2} - 1) \\ -(\frac{\sqrt{3}}{2} - 1) \\ -(\frac{\sqrt{3}}{2} - 1) \end{Bmatrix} - \begin{Bmatrix} -\delta_1 \\ 0 \\ \delta_1 \\ \delta_1 \\ \delta_1 \\ -\delta_1\frac{1}{2} \\ \delta_1\frac{1}{2} \\ \delta_1\frac{1}{2} \\ -\delta_1\frac{1}{2} \end{Bmatrix} \tag{36c}$$

where

$$\varphi_1^* = \varphi_1 + \alpha_1^A \quad (37a)$$

$$\varphi_2^* = \varphi_2 + \alpha_2^I \quad (37b)$$

$$\varphi_3^* = \varphi_3 + \alpha_3^A \quad (37c)$$

It can be seen that in the $3 \times 9 = 27$ equations there are $3 \times 5 + 2 = 17$ unknowns. The five unknowns for each pendulum are the misalignment angles, φ_i and ψ_i , the amplification constant, $a_i^{z,w}$, and the absolute deflection angles for the two normal positions, α_i^A and α_i^I . The additional two unknowns, common for all the penduli, are the angles of the tilt table, δ_1 and δ_2 . The number of equations is still larger than the number of unknowns. The following features of equations (36a) and (36b) should be noted: (1) the equations for the different penduli are coupled through δ_1 and δ_2 , and (2) solution only for the sums $\varphi_i + \alpha_i^A$ and $\varphi_i + \alpha_i^I$ can be obtained (otherwise the problem is ill-posed). Also, all the unknown angles are small and, ideally, least squares should be applied to the uncoupled systems of equations with respect to the different penduli. Therefore, first the angles δ_1 and δ_2 should be evaluated using some independent equations and then substituted into the uncoupled systems. Other independent equations are needed to calculate angles φ_i from the sums $\varphi_i + \alpha_i^A$ and $\varphi_i + \alpha_i^I$.

Evaluation of δ_1 and δ_2 —iteration

The difference equations can be constructed by subtracting the static equilibrium equations for the two normal positions A and I . Let α_i^{A-I} be the relative angle

$$\alpha_i^{A-I} = \alpha_i^A - \alpha_i^I \quad (38)$$

The normalized absolute forces \mathbf{F}_n^A and \mathbf{F}_n^I are the same and can be factored out. The new difference equation is then

$$A - I: [[T_{\alpha^A}] - [T_{\alpha^I}] + [T_{\delta,L}] - [T_{\delta,T}]] \begin{Bmatrix} 0 \\ 0 \\ 1 \end{Bmatrix} = \{\alpha_i^{A-I} \ a_i^{z,w}\} \quad (39)$$

Only the third component of the normalized force vector is non-zero, which further simplifies this equation. Since the third columns of matrices $[T_{\alpha^A}]$ and $[T_{\alpha^I}]$ are zero, their product with the force vector is a zero vector, and only the matrices $[T_{\delta,L}]$ and $[T_{\delta,T}]$ remain in equation (39). These two matrices have zero entry in the third row of the third column, and the third equation of the system is trivially satisfied. What remains from the system are the following two equations:

$$\delta_1 + \delta_2 = \alpha_1^{A-I} a_1^{z,w} \quad (40a)$$

$$-\delta_1 + \delta_2 = \alpha_2^{A-I} a_2^{z,w} \quad (40b)$$

which imply

$$\delta_1 = 0.5(\alpha_1^{A-I} a_1^{z,w} - \alpha_2^{A-I} a_2^{z,w}) \quad (41a)$$

$$\delta_2 = 0.5(\alpha_1^{A-I} a_1^{z,w} + \alpha_2^{A-I} a_2^{z,w}) \quad (41b)$$

Equations (41) require that the amplification constants $a_1^{z,w}$ and $a_2^{z,w}$ are known before angles δ_1 and δ_2 are estimated. These two constants are stable quantities and their estimate is not affected much by the changes in the misalignment angles or by angles δ_1 and δ_2 . Therefore, iteration can be performed as follows. The first approximation can be obtained by solving the difference equations assuming $\delta_1 = 0$ and $\delta_2 = 0$. These first estimates are then substituted into equations (41), solving for δ_1 and δ_2 . The new estimates of δ_1 and δ_2 are

then substituted into the difference equations whose solution gives new estimates for $a_1^{z,w}$, $a_2^{z,w}$, φ_i^* and ψ_i . The iteration is repeated as required by a preset accuracy criterion. The convergence is very fast. Accuracy of 0.01° is achieved only in few steps.

Evaluation of α_i^A and α_i^I , and φ_i

What remains is to find angles φ_i from $\varphi_1^* = \varphi_1 + \alpha_1^A$, $\varphi_2^* = \varphi_2 + \alpha_2^I$ and $\varphi_3^* = \varphi_3 + \alpha_3^A$. The equilibrium equations for the two normal positions, *A* and *I*, can be used for this purpose. Due to the particular arrangements of zeroes in the normalized force vectors \mathbf{F}_n^A and \mathbf{F}_n^I and in matrices $[T_{\varphi,\psi}]$ and $[T_\alpha]$, all φ_i and α_i drop out in the LHS of these equations, which reduce to

$$A: \begin{Bmatrix} 0 \\ 0 \\ 1 \end{Bmatrix} + \begin{Bmatrix} \psi_1 \\ -\psi_2 \\ 0 \end{Bmatrix} + \begin{Bmatrix} 0 \\ 0 \\ 0 \end{Bmatrix} + \begin{Bmatrix} \delta_2 \\ -\delta_1 \\ 0 \end{Bmatrix} = \begin{Bmatrix} a_1^{z,w} \alpha_1^A \\ a_2^{z,w} \alpha_2^A \\ a_3^{z,w} (\alpha_3^A + \alpha_3^0) \end{Bmatrix} \tag{42a}$$

and

$$I: \begin{Bmatrix} 0 \\ 0 \\ 1 \end{Bmatrix} + \begin{Bmatrix} \psi_1 \\ -\psi_2 \\ 0 \end{Bmatrix} + \begin{Bmatrix} 0 \\ 0 \\ 0 \end{Bmatrix} + \begin{Bmatrix} -\delta_1 \\ -\delta_2 \\ 0 \end{Bmatrix} = \begin{Bmatrix} a_1^{z,w} \alpha_1^I \\ a_2^{z,w} \alpha_2^I \\ a_3^{z,w} (\alpha_3^I + \alpha_3^0) \end{Bmatrix} \tag{42b}$$

Recalling the expression for α_3^0 (equations (21)), from the above equations it follows that

$$\alpha_1^A = (\psi_1 + \delta_2)/a_1^{z,w} \tag{43a}$$

$$\alpha_2^A = -(\psi_2 + \delta_1)/a_2^{z,w} \tag{43b}$$

$$\alpha_3^A = 0 \tag{43c}$$

$$\alpha_1^I = (\psi_1 - \delta_1)/a_1^{z,w} \tag{44a}$$

$$\alpha_2^I = -(\psi_2 + \delta_2)/a_2^{z,w} \tag{44b}$$

$$\alpha_3^I = 0 \tag{44c}$$

It is seen that the first-order analysis implies that the angles of deflection, when the instrument is in normal positions for the first two penduli (*L* and *T*), are equal to the effective misalignment angles ψ_1 and ψ_2 for the particular normal position, while for the third pendulum (*V*) those angles are zero. A corollary of this is that the difference $\alpha_3^A - \alpha_3^I = 0$, and this should be seen in the tilt test results. Indeed, in all of our results for the Los Angeles Strong Motion Network, there were noticeable jumps between the traces for the two normal positions (e.g., Positions *E* and *F*, or *E'* and *F'*) only for the *L* and *T* penduli.²¹

Finally, the misalignment angles φ_i are obtained from

$$\varphi_1 = \varphi_1^* - \alpha_1^A \tag{45a}$$

$$\varphi_2 = \varphi_2^* - \alpha_2^I \tag{45b}$$

$$\varphi_3 = \varphi_3^* - \alpha_3^A \tag{45c}$$

where φ_i^* are as defined by equation (39).

DISCUSSION AND CONCLUSIONS

A mathematical model was presented for a typical accelerograph with pendulum like transducers under the action of static or dynamic forces, considering large deflections and misaligned transducers. Linearizing the

equations eliminates one of the three misalignment angles (θ —representing rotation in the plane which contains the pendulum boom and its pivot axis) which contributes only second-order terms. The presented model can be generalized to other accelerographs with pendulum-like transducers.

The static equilibrium equations and a static tilt test were used to formulate an algorithm for finding the misalignment angles and the amplification constants (the inverse problem). The static tilt test consists of a sequence of measurements which lead to an overdetermined system of equations for each transducer. The equations are coupled through the angles of the tilt table, which is not perfectly horizontal. In the proposed algorithm, the systems of equations are solved independently for each transducer by the singular-value decomposition method.²⁴ The systems are decoupled by substituting estimates for the angles of the tilt table, which are improved by iteration. Therefore, adding the tilt table angles as unknowns did not increase the number of unknowns in the numerical inversion. The high accuracy of reading the trace positions on the film via a digital scanner and the combination of iteration and numerical inversion of an overdetermined system make the algorithm very stable.²¹ The procedure of Wong and Trifunac¹⁹ did not consider nonhorizontal tilt table, and solved for the unknowns one by one from selected difference equations. The new algorithm (and the interactive computer program TILT²¹), based on least-squares solution of an overdetermined system of equations (nine equations and three unknowns), is more accurate, introduces redundancy and flexibility, and is convenient for routine processing of tilt test results. Results of tilt tests for a typical strong motion array and analysis of the overall accuracy (especially on the estimates of sensitivity) are presented in Todorovska *et al.*^{21,22}

Another source of error (yet intractable) in measuring strong ground motion is earthquake generated tilting of the recording instrument. Such tilting in the gravity field will cause larger errors in the recorded horizontal accelerations, and smaller errors in the recorded vertical accelerations (this is analogous to the effect of the tilt table angles on the pendulum deflection when the instrument is horizontal, which is significant only for the L and T transducers). These errors may be significant near the source of intermediate and large earthquakes.

REFERENCES

1. M. D. Trifunac and V. W. Lee, 'Automatic digitization and processing of strong-motion accelerograms, Part I and II', *Report No. CE 79-15*, Dept. of Civil Eng., Univ. of Southern California, Los Angeles, California, 1979.
2. V. W. Lee and M. D. Trifunac, 'Automatic digitization and processing of accelerograms using PC', *Report No. CE 90-03*, Dept. of Civil Eng., Univ. of Southern California, Los Angeles, California, 1990.
3. M. D. Trifunac and D. E. Hudson, 'Laboratory evaluation and instrument corrections of strong motion accelerographs', Report EERL 70-04, Earthquake Eng. Res. Lab., Calif. Inst. of Tech., Pasadena, California, 1970.
4. M. D. Trifunac, 'Zero baseline correction of strong motion accelerograms', *Bull. Seism. Soc. Amer.* **61**, 1201–1211 (1971).
5. M. D. Trifunac, F. E. Udvardia and A. G. Brady, 'Analysis of errors in digitized strong motion accelerograms' *Bull. Seism. Soc. Amer.* **63**, 157–187 (1973).
6. M. D. Trifunac and V. W. Lee, 'A note on the accuracy of computed ground displacements from strong motion accelerograms', *Bull. Seism. Soc. Amer.* **64**, 1209–1219 (1974).
7. V. W. Lee, A. Amini and M. D. Trifunac, 'Noise in earthquake accelerograms', *J. Engng. Mech. ASCE* **108**, 1121–1129 (1982).
8. A. Amini and M. D. Trifunac, 'Optimum frequency and damping for optically recording strong motion accelerographs', *Soil Dyn. Earthquake Engng.* **1**, 189–194 (1982).
9. A. Amini and M. D. Trifunac, 'Analysis of a feed-back transducer', *Report No. CE 83-03*, Dept. of Civil Engng, Univ. of Southern California, Los Angeles, California, 1983.
10. A. Amini and M. D. Trifunac, 'Analysis of Force Balance Accelerometer', *Soil Dyn. Earthquake Engng* **4**, 82–90 (1985).
11. D. K. Markus, K. Moslem and M. D. Trifunac, 'A note on controlling the optical density of analog film records in strong motion accelerographs', *Soil Dyn. Earthquake Engng* **4**, 31–34 (1985).
12. A. Amini, R. L. Nigbor and M. D. Trifunac, 'A note on the noise amplitudes in some strong motion accelerographs', *Soil Dyn. Earthquake Engng.* **6**, 180–185 (1987).
13. A. Amini, O. Hata and M. D. Trifunac, 'Experimental analysis of R/L-1, Chinese Force Balance Accelerometer', *Earthquake Engng. Engng. Vib.* **11**, 77–88 (1991).
14. E. I. Novikova and M. D. Trifunac, 'Instrument correction for the coupled transducer-galvanometer systems', *Report No. CE 91-02*, Dept. of Civil Engng, Univ. of Southern California, Los Angeles, California, 1991.
15. E. I. Novikova and M. D. Trifunac, 'Digital instrument response correction for the Force Balance Accelerometer', *Earthquake Spectra* **8**, 429–442 (1992).
16. V. W. Lee and M. D. Trifunac, 'Strong Earthquake Ground Motion Data in EQINFOS: Part I', *Report No. CE 87-01*, Dept. of Civil Eng., Univ. Southern California, Los Angeles, California, 1987.

17. V. W. Lee and M. D. Trifunac, 'EQINFOS (the Strong Motion Earthquake Data Information System)', *Report No. CE 82-01*, Dept. of Civil Eng., Univ. Southern California, Los Angeles, California, 1982.
18. R. I. Skinner and W. R. Stephenson, 'Accelerograph calibration and accelerogram correction', *Earthquake Engng. Struct. Dyn.* **2**, 71–86 (1973).
19. H. L. Wong and M. D. Trifunac, 'Effects of cross-axis sensitivity and misalignment on the response of mechanical-optical accelerographs', *Bull. Seism. Soc. Amer.* **67**, 929–956 (1977).
20. M. D. Trifunac and M. I. Todorovska, Nonlinear soil response—1994 Northridge, California, earthquake, *J. Geotech. Engng. ASCE* **122**, 725–735 (1996).
21. M. I. Todorovska, E. I. Novikova, M. D. Trifunac and S. S. Ivanović, 'Correction for misalignment and cross-axis sensitivity of strong earthquake motion recorded by SMA-1 accelerographs', *Report No. CE 95-06*, Dept. of Civil Engrg, Univ. of Southern California, Los Angeles, California, 1995.
22. M. I. Todorovska, E. I. Novikova, M. D. Trifunac and S. S. Ivanović, Advanced sensitivity calibration of the Los Angeles Strong Motion Array, *Earthquake Engng. Struct. Dyn.* **27**, 1053–1068 (1998).
23. L. Meirovitch, *Elements of Vibration Analysis*, McGraw-Hill, New York, 1975.
24. W. H. Press, B. P. Flannery, S. A. Teukolsky and W. T. Vetterling, *Numerical Recipes*, Cambridge University Press, Cambridge, MA, 1989.